Estimation of Wind Tunnel Corrections Using Potential Models

Ionut BUNESCU*,[1,2], Sterian DANAILA[2], Mihai-Victor PRICOP[1], Adrian DINA[1,2]

*Corresponding author
*,[1]INCAS – National Institute for Aerospace Research "Elie Carafoli",
B-dul Iuliu Maniu 220, 061126 Bucharest, Romania,
bunescu.ionut@incas.ro*, pricop.victor@incas.ro, dina.adrian@incas.ro
[2]"POLITEHNICA" University of Bucharest, Faculty of Aerospace Engineering,
Department of Aerospace Sciences "Elie Carafoli",
Str. Polizu 1-7, sector 1, 011061 Bucharest, Romania,
sterian.danaila@gmail.com

DOI: 10.13111/2066-8201.2019.11.1.4

Received: 07 January 2019/ Accepted: 05 February 2019/ Published: March 2019

International Conference of Aerospace Sciences "AEROSPATIAL 2018"
25 - 26 October 2018, Bucharest, Romania, (held at INCAS, B-dul Iuliu Maniu 220, sector 6)
Section 1 – Aerodynamics

Abstract: *The evaluation of the tunnel correction remains an actual problem, especially for the effect of tunnel walls. Even if the experimental campaign meets the basic similitude criteria (Mach, Reynolds etc.), the wall effect on the measured data is always present. Consequently, the flow correction due the limited by walls must be evaluated. Solid wall corrections refer to the aerodynamic interference between the experimental model and the walls of the wind tunnel. This interaction affects the measured forces and implicitly the angle of attack. Usually, these effects are introduced through semi-empirical correction factors which change the global measured forces. The present paper refers to the mathematical and numerical modeling of aerodynamic interferences between the experimental model and the solid walls based on the potential flow model. The main goal is to asses a method allowing an estimate of the corrections for each configuration with a minimum computational resource.*

Key Words: *solid walls corrections, wall interference, panel methods, method of images*

1. INTRODUCTION

Although there are high accuracy methods to estimate these corrections, there is a need to find a method that delivers good results without using a large amount of resources. Among the previous studies on using the potential model to estimate the wall interferences we quote the AGARD reports [6] and [7].

Neglecting the fluid viscosity and assuming the hypothesis of a stationary and irrotational incompressible flow, the governing flow equations reduce to Laplace equation for the velocity potential.

The associated boundary conditions at solid walls turn into the slip condition along the walls. If the resolution of Laplace equation is based on the superposition of distributed

different particular solutions (source potential, vortex potential, doublet potential etc.) the wall effect must be simulated by a series of images in order to satisfy the slip boundary condition on the tunnel walls.

Applications concern the two-dimensional flow around NACA 0012 airfoil and the three-dimensional flow around a rectangular wing both in a rectangular wind tunnel.

2. MATHEMATICAL MODEL AND METHODS USED

As we have already mentioned, the adopted mathematical model is the potential model, extensively described in [1].

The numerical solution is based on the panel method, where the source, vortices and doublet are distributed along the configuration surface.

For the two-dimensional case we will use a Linear Strength Vortex Method (LSVM), and for the three-dimensional case, the Higher Order Panel Methods based on the quadratic intensity doublet variation and on linear intensity sources distribution [1, 2, 12].

2.1 The two-dimensional case

For this case, we chose a panel-based method that uses linear vortex distributions on the outline, because this method is much closer to experimental results than any other:

$$\gamma(x) = \gamma_0 + \gamma_1 (x - x_1) \tag{1}$$

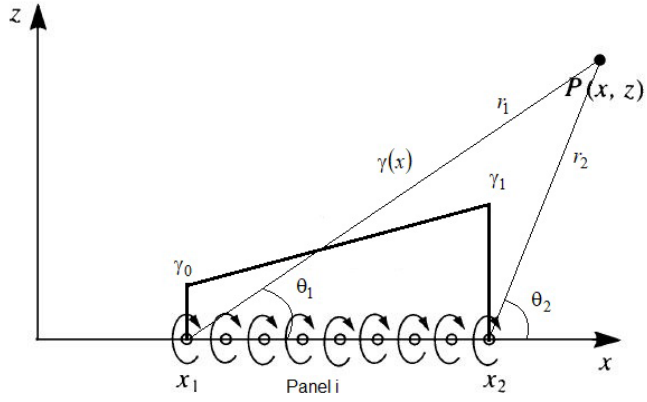

Fig. 1 Description of panel elements

We will divide this problem into two problems in which we have a constant intensity vortex distribution and a linear intensity vortex distribution that goes from zero; therefore the potential given by the two types of vortex distributions is:

$$\phi_c = -\frac{\gamma_0}{2\pi}\left[(x - x_1)\theta_1 - (x - x_2)\theta_2 + \frac{z}{2}\ln\frac{r_1^2}{r_2^2}\right]$$

$$\phi_l = -\frac{\gamma_1}{2\pi}\left(\frac{xz}{2}\ln\frac{r_1^2}{r_2^2} + \frac{z}{2}(x_1 - x_2) + \frac{x^2 - x_1^2 - z^2}{2}\theta_1 - \frac{x^2 - x_2^2 - z^2}{2}\theta_2\right) \tag{2}$$

where x_1, x_2 are the coordinates of the panel corners, θ_1, θ_2 are the angles between the panel and the line joining the end of the panel with the point of colocation and r_1, r_2 are the distance between the end of the panel and the colocation point.

Therefore the potential given by the two superposed distributions is:

$$\phi_t = \phi_l + \phi_c = -\frac{\gamma_1}{2\pi}\left(\frac{xz}{2}\ln\frac{r_1^2}{r_2^2} + \frac{z}{2}(x_1 - x_2) + \frac{x^2 - x_1^2 - z^2}{2}\theta_1 - \frac{x^2 - x_2^2 - z^2}{2}\theta_2\right) - \ldots$$
$$\ldots - \frac{\gamma_0}{2\pi}\left[(x - x_1)\theta_1 - (x - x_2)\theta_2 + \frac{z}{2}\ln\frac{r_1^2}{r_2^2}\right] \tag{3}$$

and the induced velocity components result as:

$$u_t = \frac{\partial\phi_t}{\partial x} = +\frac{\gamma_1}{4\pi}\left(z\ln\frac{r_1^2}{r_2^2} - 2x(\theta_2 - \theta_1)\right) + \frac{\gamma_0}{2\pi}(\theta_2 - \theta_1)$$
$$w_t = \frac{\partial\phi_t}{\partial z} = -\frac{\gamma_1}{4\pi}\left(x\ln\frac{r_1^2}{r_2^2} + (x_1 - x_2) + 2z(\theta_2 - \theta_1)\right) - \frac{\gamma_0}{4\pi}\ln\frac{r_2^2}{r_1^2} \tag{4}$$

Note that induced velocities result from calculating some influence coefficient matrices and then calculating the singularity intensities by which we can find the velocities induced by each singularity at each point on the contour of the model.

$$[\boldsymbol{A}]\cdot\{\boldsymbol{\gamma}\} = \{\boldsymbol{b}\} \tag{5}$$

where matrix [***A***] is the influence coefficient matrix with $a_{i,j}$ components, and {***b***} is the vector of free terms, right-hand side, with b_i elements:

$$a_{i,j} = (u, w)_{i,j}\cdot\boldsymbol{n}_i$$
$$b_i = -(U_\infty, W_\infty)\cdot(\cos\alpha_i, -\sin\alpha_i), \tag{6}$$

$\mathbf{n}_i$ is the normal vector at the panel, and α_i is the angle of seating's panel.

2.2 The three-dimensional case

The same can be found for the three-dimensional case using a distribution of the linear intensity source and a quadratic doublet distribution over the panel:

$$\Delta\phi_S = \sigma_0 + \sigma_x x + \sigma_y y$$
$$\Delta\phi_D = \mu_0 + \mu_x x + \mu_y y + \mu_{xy} xy + \mu_{xx} x^2 + \mu_{yy} y^2 \tag{7}$$

These issues are extensively dealt in [2] and [12] for this case. Note that finally a system of equation needs to be solved:

$$[\boldsymbol{A}]\cdot\{\boldsymbol{\mu}\} = -[\boldsymbol{B}]\{\boldsymbol{\sigma}\} \tag{8}$$

where [**A**], [**B**] – represent the influence coefficients matrices and {**σ**},{**μ**} are the vector of the source and doublet singularities.

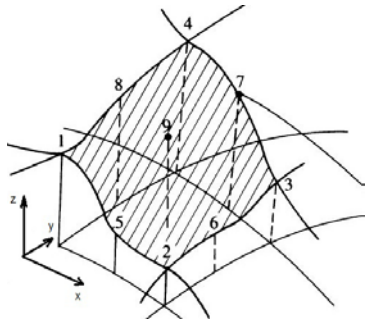

Fig. 2 Distribution of singularities over the panel

By finding the velocity distribution on the contour of the model, we can immediately find the pressure distributions and coefficients. In addition, in order to quantify the effect of walls, the method of images (IM) is also used after finding the singularity intensities. The method of images is described in more detail in works [9] and [14]; this method is a way of calculating the effect of some boundaries on the computing area by placing singularities (called images) in mirror to the boundaries of the computing domain (the walls of the wind tunnel).

The positioning of the images is iterative, that is, for the two-dimensional case, we have a mirror image to the top border and a mirror image to the lower border; these newly created images are assigned in turn to another image to the remaining borders, for the top image a mirror image is created from the bottom boundary and vice versa, continuing the process until infinite. Finally, we obtain an array with alternate inverted images for which the effect is calculated on the airfoil contour. Obviously, the mirror images which are farther away from the airfoil contour have a diminished interference effect.

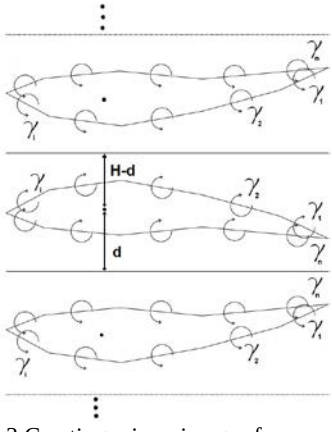

Fig. 3 Creating mirror images for a profile

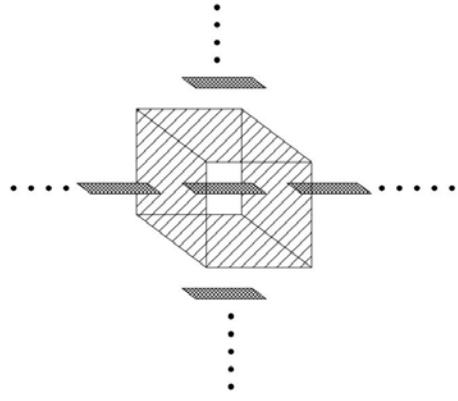

Fig. 4 Creating mirror images for a wing

The law of mirror image location is given by the formula below:

$$z_i = (-1)^i \cdot z \pm \left(zf_{i-i} + \begin{cases} \text{mod}(i,2)(H-d) + (1-\text{mod}(i,2))d \\ \text{mod}(i,2)d + (1-\text{mod}(i,2))(H-d) \end{cases} \right) \tag{9}$$

where “mod” function represents modulo operation which finds the remainder after division of one number (i) by another (2), z is vertical coordinate of airfoil, i indicate the number of image, H is the hight of wind tunnel and d is the distance between the airfoil and the wind tunnel’s floor. For the three-dimensional case, we have both a vertical alignment to the top

and bottom boundaries just like in two-dimensional case, but we also have a lateral position relative to the lateral borders, thus obtaining an images board.

3. RESULTS

For the two-dimensional case, we calculated the distribution of the pressure coefficients on the airfoil contour at 2º incidence and the dependence of the lift coefficients on the incidence, with the indication that the profile is meshed into 80 panels and H = 2m, d=1m. Therefore the results obtained are as follows:

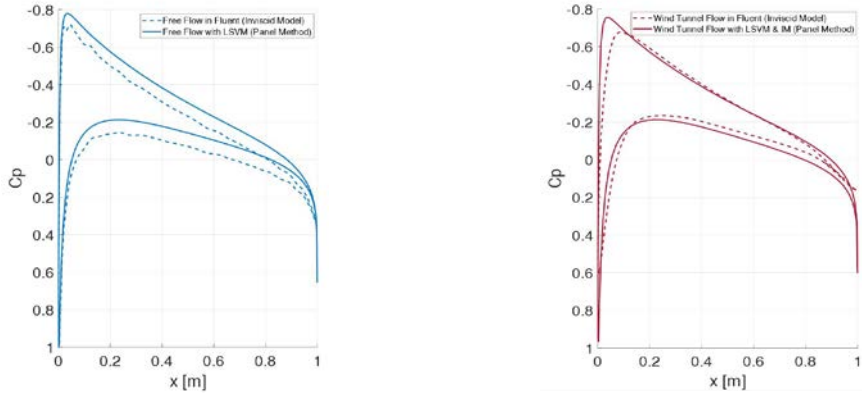

a) b)

Fig. 5 a) Pressure coefficients distribution along the chord for a free flowing NACA 0012 profile [2deg], b) Pressure coefficients distribution along the chord for a NACA 0012 profile in wind tunnel flow [2deg]

In addition, for verification with the Fluent program (Inviscid Model) we have calculated the pressure coefficients distribution along the chord and the lift coefficients dependence on the incidence in order to compare by the estimation method using the potential model. It is worth noting that there are appreciable differences between the two methods of estimating the corrections; what matters is that the difference between the two methods for each case is comparable, so the estimation of the corrections can be sufficiently precise. From the picture below it also can be seen that the differences between the two pairs of curves are very small so it is possible to use more simple potential models instead of the more complex models of high accuracy.

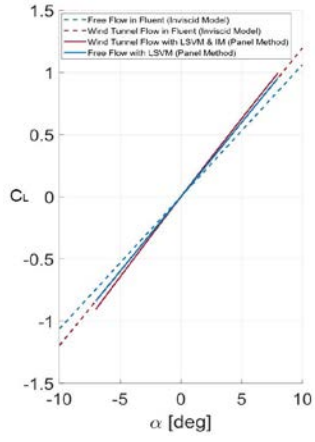

Fig. 6 The dependency curve C_L - α

From Fig. 7, we notice that the process converges with the increase of the number of images used, given that the vertical velocity at wall is null when the wind tunnel walls are solid and do not allow the passage of the air flow.

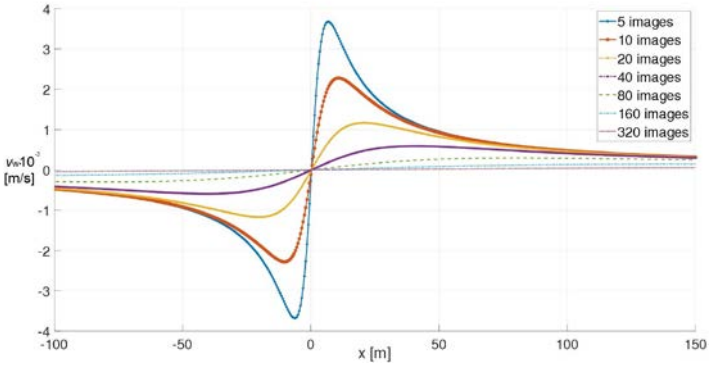

Fig. 7 The effect of the number of mirror images on the vertical speed at the wall

For the three-dimensional case we calculated the distribution of the pressure coefficients on the wing surface at an incidence of 2º and the dependence of the lift coefficients on the angle of attack, noting that the wing is meshed in 30 panels along the chord and another 10 panels along the span. Therefore, the results obtained are given in the figures below.

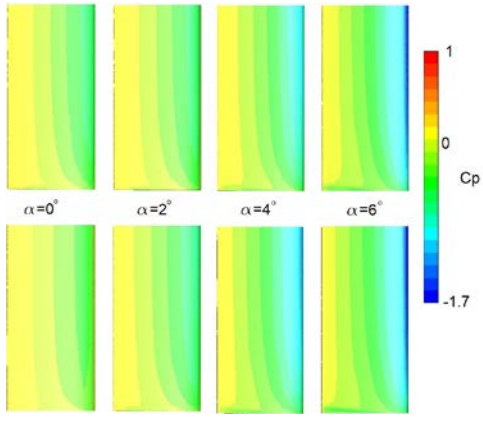

Fig. 8 The pressure coefficients distribution over the upper surface of wing at various angles of attack (the upper row - the free flow, the bottom row - the flow in the tunnel)

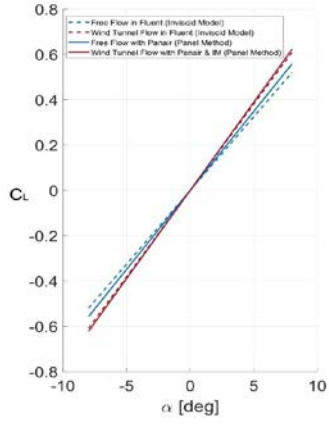

Fig. 9 Dependence of lift coefficient on the angle of attack (comparison between free flow and flow in the tunnel)

From Fig. 8 we can see small differences in both the distribution shape of the of the pressure coefficients and their values. Although in the figure above, free flow images have a larger depression, the wing load coefficient is lower for limited flow (in the wind tunnel), as seen in the figure Fig. 9. In order to be able to precisely compare the obtained results, we define a correction coefficient representing the ratio of the lift coefficient of the profile in the free flow and that of the profile in the wind tunnel:

$$K_{C_L} = \frac{C_{L_{free}}}{C_{L_{WT}}} \tag{10}$$

Thus we obtain the following values for both cases, airfoil and wing, in the wind tunnel and in the free flow at a two-degree incidence:

Table 1. Comparing the results obtained for a NACA 0012 airfoil (2º angle of attack)

-	LSVM & IM (Panel Method)	Fluent (Inviscid Model)
C_{Lfree} [airfoil]	0.23965	0.22721
C_{LWT} [airfoil]	0.25331	0.23842
C_{Lfree} [wing]	0.14207	0.14081
C_{LWT} [wing]	0.16541	0.1582
K_{CL} [airfoil]	**0.94607**	**0.95298**
K_{CL} [wing]	**0.86103**	**0.89075**

We can observe that the percentage relative error doesn't exceed 5%, so we can admit that the method used can be applied with confidence to estimate wall corrections in exchange for a high fidelity computation method for an inviscid flow.

We mention that :

$$C^e_{L_{free}} = C^e_{L_{WT}} - \left(C^n_{L_{WT}} - C^n_{L_{free}}\right) \tag{11}$$

$$C^e_{L_{free}} = C^e_{L_{WT}} - C^n_{L_{WT}}\left(1 - K^n_{CL}\right) \tag{12}$$

where C_L represents the lift coefficient, "e" refers to experimental coefficient, "*n*" refers to numerical coefficient, "free" refers to free flow and "WT" refers to wind tunnel flow.

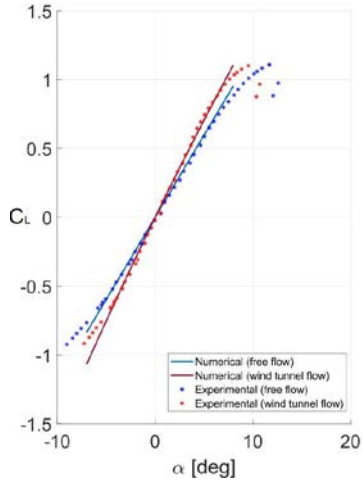

Fig. 10 Estimating corrected lift coefficients using experimental raw lift coefficients and numerical lift coefficients for both cases (free flow and wind tunnel flow)

We observe that it's possible to estimate corrected lift coefficients using equation (11) with experimental raw lift coefficients and numerical lift coefficients of free flow and wind tunnel flow.

4. CONCLUSIONS

As an overview of the present paper, we can say that the objective has been achieved, the panel method (using potential models) combined with mirror image methods can estimate the tunnel corrections to a certain extent; also, the time for making calculations is much lower than simulations made in more complex computing programs.

We also showed that the difference between the two methods of estimating wall corrections is small, generally does not exceed 5%, which makes the method applicable in

engineering to estimate wall corrections accurately enough and in relatively short time on more complex computing models. Estimating solid wall corrections using these methods is individual to each model and far superior to standard wall corrections.

In conclusion, it is possible to make quite precise corrections using these methods, all the effort being much smaller than in the case of simulations in complex computing programs; however there are limitations and for several series of images the calculation time increases. Future work is to find ways to quickly and accurately estimate tunnel corrections, resulting in more accurate experimental results and developing scope; for instance we can talk about optimizing aerodynamic model experimentation (fluid flow, pressure, speed, etc.).

ACKNOWLEDGEMENT

This paper is a part of the work in the bachelor's thesis *"Estimation of Wind Tunnel Corrections Using Potential Models"*, by Ionut BUNESCU, awarded with the "Nicolae TIPEI" prize during **The International Conference of Aerospace Sciences "AEROSPATIAL 2018"**, 25 - 26 October 2018, Bucharest, Romania, organized by the INCAS – National Institute for Aerospace Research "Elie Carafoli".
I would like to express my deep gratitude to Professor PhD. Eng. Sterian DANAILA and Eng. Mihai-Victor PRICOP, my research supervisors, for their patient guidance and useful critiques of this research work. I would also thanks to Professor Sever TIPEI the son of Nicolae TIPEI and to the INCAS institute, led by PhD. Eng. Catalin NAE, for their support and encouragement for young researchers.

REFERENCES

[1] S. Dănăilă and C. Berbente, *Metode numerice în dinamica fluidelor*, Romanian Academy Press, Bucharest, 2003.
[2] J. Katz and A. Plotkin, *Low-Speed Aerodynamics*, Cambridge University Press, New York, 2001.
[3] N. Tomescu, *Aerodinamică experimentală*, Polytechnic Institute of Bucharest, Vol. **1**, Bucharest, 1991.
[4] S. Wiriadidjaja, R. Mohd, F. Romili and O. Ariff, Aerodynamic Interference Correction Methods Case: Subsonic Closed Wind Tunnels, *Applied Mechanics and Materials*, Vol. **225**, pp 60- 66, 2012.
[5] D. Althaus, *Tunnel- Wall Corrections at the Laminar Wind Tunnel*, https://www.iag.uni-stuttgart.de/abteilungen/laminarwindkanal/pdf_laminar/corrections.pdf.
[6] B. F. R. Ewald, *Wind Tunnel Wall Corection*, AGARD -AG-336, Canada Communication Group, 1998.
[7] * * * *Wall interference in wind tunnels*, AGARD -CP-335, 1982.
[8] P. Rebuffet, *Aerodynamique expérimentale*, Troisiéme édition, pp 131-143, Dunon, Paris, 1969.
[9] J. Barlow, W. Rae and A. Pope, *Low speed wind tunnel testing*, Third Edition, JohnWiley & Sons, New York, 1999.
[10] C. Tropea, L. A. Yarin and F. J. Foss, *Handbook of experimental fluid mechanics*, Springer, 2007.
[11] K. Sidwell, P. Baruah, J. Bussoletti, R. Medan, R. Conner, Rand D. Purdon, *PANAIR – A Computer Program for Predicting Subsonic or Supersonic Linear Potential Flows About Arbitrary Configurations Using a Higher Order Panel Method*, Vol. **II**, Version 3.0, NASA Contractor Report 3252,1990.
[12] A. Magnus and M. Epton, *PANAIR – A Computer Program for Predicting Subsonic or Supersonic Linear Potential Flows About Arbitrary Configurations Using a Higher Order Panel Method*, Vol. **I**, Version 1.1, NASA Contractor Report 3251, 1981.
[13] T. A. Abdullah, Z. Petrovic, Z. Stefanovic, I. Kostic and J. Isakovic, *Two- Dimensional wind tunnel measurement corrections by the singularity method*, Tehnicki Vjesnik, **22**(3):557-565, June 2015, DOI: 10.17559/TV-20140214114718.
[14] * * * *Method of images*, Avaibele at https://en.wikipedia.org/wiki/Method_of_images.
[15] L. L. Erickson, *Panel Methods – An Introduction*, Nasa Technical Paper 2995,Moffet Field, California 1990.